ISSN 1392 - 1207. MECHANIKA. 2009. Nr.2(76)

Study of resonant vibrations shapes of the beam type piezoelectric actuator with preloaded mass

D. Mažeika*, R. Bansevičius**
**Vilnius Gediminas Technical University, Saulėtekio 11, 10223 Vilnius, Lithuania, E-mail: Dalius.Mazeika@fm.vgtu.lt*
***Kaunas University of Technology, Kęstučio 27, 44312 Kaunas, Lithuania, E-mail: Ramutis.Bansevicius@cr.ktu.lt*

1. Introduction

Piezoelectric actuators are widely used in high precision mechanical systems such as positioning devices, manipulating systems, control equipment and etc. Piezoelectric actuators have advanced features such as high resolution, short response time, compact size, and good controllability [1, 2]. Vibration amplitudes of the bulk piezoceramic element usually are at range of nanometers, so very often piezoceramics is combined with amplifier mechanism to enlarge stroke of the actuator [3-5]. However some problems appear applying amplifier mechanisms, i.e. difference between wave propagation speed of piezoceramics and amplifier, accuracy issues of gluing and mounting and etc.

In general many design principles of piezoelectric actuators are proposed [3, 5, 6]. Summarizing the following types of piezoelectric actuators can be specified: traveling wave, standing wave, hybrid transducer, and multimode vibrations actuators [3, 5].

Piezoelectric actuator of multimode vibrations type is presented and analyzed in this paper. It composes of bulk piezoceramic beam with a single mass at one of the ends. No vibrations amplifier is used. Usual approach to achieve multimode vibrations at resonant frequency is to find particular geometrical parameters of the actuator [5]. But in some cases it is not possible due to the technical requirements. By adding external mass element we can change dynamic characteristics of the actuator and multimode vibrations can be obtained at resonant frequency without changing geometry of the actuator. Numerical modeling of piezoelectric actuator was carried out to evaluate operating principle and to investigate the mass influence on vibration shapes of the actuator and on parameters of elliptical trajectories of the contact point.

2. Concept of piezoelectric actuator

Configuration of actuator includes two parts: piezoceramic beam and single steel mass that is glued at one of the ends of beam (Fig. 1, a). Polarization vector of piezoceramic beam is oriented along the thickness and piezoelectric effect d_{31} is used for the actuation. Electrodes are located at the bottom of the beam and are divided into two equal sections (Fig. 1, b). This type of electrode pattern is used to realize two different excitation schemes and to obtain direct and reverse motion of the slider.

Operation of the actuator is based on using longitudinal and flexural multimode resonant vibrations of the actuator. Two separate resonant frequencies are used for actuation. Superposition of the 1st longitudinal mode and the nearest flexural mode is used to obtain elliptical trajectory of contact point and to achieve direct motion of the slider. Excitation scheme when voltage with the same phase is applied on the both electrodes is used in this case (Fig. 1, b). Superposition of the 2nd longitudinal mode and the nearest flexural mode is used to obtain reverse motion of the slider. Excitation voltage has phase difference by π on different electrodes in this case (Fig. 1, b). Flexural vibration mode participating in superposition depends on *h/l* ratio of the actuator.

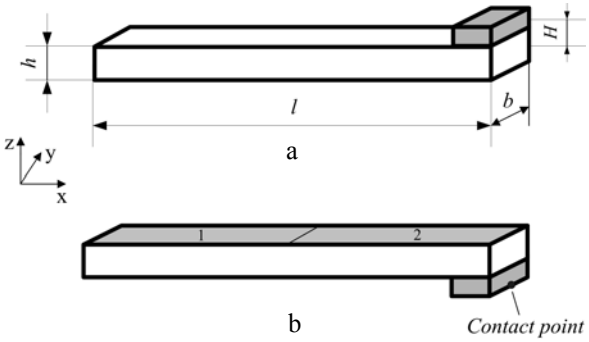

Fig. 1 Principle scheme of the actuator: a) general view; b) pattern of electrodes

Dimensions of the analyzed piezoelectric actuator (Fig. 1, a) correspond to the requirements of classical beam, so the equations of beam oscillations can applied. Therefore longitudinal oscillations of the actuator with preloaded mass can be written as follows

$$\left(m+m_{pr}\left(x\right)\right)\frac{\partial^2\xi}{\partial t^2}-\frac{\partial}{\partial x}\left(EA\frac{\partial\xi}{\partial x}\right)+C_l\left(x,t\right)=F_{piez}sin\Omega t \quad (1)$$

where

$$F_{piez}=Ube_{31} \quad (2)$$

and m is mass of piezoceramic beam, m_{pr} is preloded mass, ξ is a function of longitudinal displacement, E is elastic modulus of piezoceramics, A is cross-section area of beam, C_l is damping function, U is voltage, b is the width of beam, e_{31} is piezoelectric coefficient, Ω excitation frequency, t is the time. Equation of flexural oscillations of the actuator can be written as

$$\left(m+m_{pr}\left(x\right)\right)\frac{\partial^2\zeta}{\partial t^2}+\frac{\partial^2}{\partial x^2}\left(EI\frac{\partial^2\zeta}{\partial x^2}\right)+$$

$$+C_f\left(x,t\right)=\frac{\partial^2 Msin\Omega t}{\partial x^2} \quad (3)$$

where ζ is function of flexure displacements, I is inertia moment of cross-section, C_f is damping function, M is inertia moment of preloaded mass and can be written as

$$M = F_{piez} H \tag{4}$$

where H is distance from the beam middle line to the mass center of the single steel mass.

Solution of Eq. 1 and 3 defines the trajectory of contact point movement and can be written in the following form [7, 8]

$$\xi(x,t) = \sum_{n=1}^{\infty} e^{-\alpha_n t} \left[G_n(x) + T_n(t) \right] \tag{5}$$

$$\zeta(x,t) = \sum_{n=1}^{\infty} \left[e^{-\alpha_n t} H(\overline{\omega}_n, t) + Y_n(\overline{\omega}_n, \alpha_n, t) \right] \zeta_n(x) \tag{6}$$

here

$$\left. \begin{aligned} H(\overline{\omega}_n, t) &= \left(A_n \sin \overline{\omega}_n t + B_n \cos \overline{\omega}_n t \right) \\ \overline{\omega}_n &= \sqrt{\omega^2 - \alpha^2} \end{aligned} \right\} \tag{7}$$

where G_n and T_n are harmonic functions, A_n and B_n are coefficients, obtained from initial conditions and $Y(\overline{\omega}_n, \alpha_n, t)$ is integral function, $\zeta_n(x)$ is flexural modal shape.

Referring to the Eq. 1 and 3 it can be seen that vibrations of the actuator depend on the preloaded mass value and its location on the actuator.

3. FEM modeling of the actuator

Finite element method was used to perform numerical modeling of the actuator. It was used to carry out modal frequency and harmonic response analysis and to calculate trajectories of contact point (Fig. 1, b) movements. Basic dynamic equation of the piezoelectric actuator are derived from the principle of minimum potential energy by means of variational functionals and can be written as follows [9-11]

$$\left. \begin{aligned} [M]\{\ddot{u}\} + [C]\{\dot{u}\} + [K]\{u\} + [T]\{\varphi\} &= \{F\} \\ [T]^T \{u\} - [S]\{\varphi\} &= \{Q\} \end{aligned} \right\} \tag{8}$$

where [M], [K], [T], [S], [C] are matrices of mass, stiffness, electro elasticity, capacity, damping respectively; $\{u\}, \{\phi\}, \{F\}, \{Q\}$ are vectors of nodes displacements, potentials, structural mechanical forces and charge.

Driving force of the piezoelectric actuator is obtained from piezoceramical element. Finite element discretization of this element usually consists of a few layers of finite elements. Therefore nodes coupled with electrode layers have known potential values in advance and nodal potential of the remaining elements are calculated during the analysis. Dynamic equation of piezoelectric actuator in this case can be expressed as follows [11, 12]

$$\left. \begin{aligned} [M]\{\ddot{u}\} + [C]\{\dot{u}\} + [K]\{u\} + [T_1]\{\phi_1\} + [T_2]\{\phi_2\} &= \{F\} \\ [T_1]^T \{u\} - [S_{11}]\{\phi_1\} - [S_{12}]\{\phi_2\} &= \{Q_1\} \\ [T_2]^T \{u\} - [S_{12}]^T \{\phi_1\} - [S_{22}]\{\phi_2\} &= \{0\} \end{aligned} \right\} \tag{9}$$

here

$$\left. \begin{aligned} [T] &= [T_1 \quad T_2] \\ [S] &= \begin{bmatrix} S_{11} & S_{12} \\ S_{12}^T & S_{22} \end{bmatrix} \end{aligned} \right\} \tag{10}$$

where $\{\varphi_1\}\{\varphi_2\}$ are accordingly vectors of nodal potentials known in advance and calculated during numerical simulation.

Natural frequencies and modal shapes of the actuator are derived from the modal solution of the piezoelectric system [11, 12]

$$det\left(\left[K^* \right] - \omega^2 [M] \right) = \{0\} \tag{11}$$

where [K^*] is modified stiffness matrix and it depends on nodal potential values of the piezoelements.

Harmonic response analysis of piezoelectric actuator is carried out applying sinusoidal varying voltage on electrodes of the piezoelements. Structural mechanical loads are not used in our case so $\{F\} = \{0\}$. Equivalent mechanical forces are obtained because of inverse piezoefect and can be calculated as follows [11, 12]

$$\{F\} = -[T]\{\varphi_1\} \tag{12}$$

here

$$\{\phi_1\} = \{U\} \sin(\omega_k t) \tag{13}$$

where $\{U\}$ is vector of voltage amplitudes, applied on the nodes coupled with electrodes. Refer to Eqs. (9), (12), (13) the vector of mechanical forces can be calculated as follows

$$\{F_{eq}\} = \left([T_2][S_{22}]^{-1}[T_2]^T - [T_1] \right) \{U\} \sin \omega_k t \tag{14}$$

Results of structural displacements of the piezoelectric actuator obtained from harmonic response analysis are used for determining the trajectory of contact point movement.

4. Results of numerical study

Numerical study of piezoelectric actuator was performed to investigate vibration shapes and trajectories of contact point motion through the modal and harmonic response analysis. FEM package ANSYS was employed for the simulation. Three dimensional finite element model was built and the following dimensions of the actuator have been used: l = 0.05 m, b = 0.01 m, h = 0.003 m, H = 0.003 m and m_{pr} = 0.114 kg. PZT-8 piezoceramics was used and constant material damping was assumed in the model.

Modal analysis of piezoelectric actuator was done to find applicable modal shapes and natural frequencies of the actuator. Actuator has multimode vibration shapes due to the preloaded mass, so criteria for applicable modal shape selection was dominating longitudinal displacement at the frequencies close to the first and second longitudinal mode. Modal shapes at 30.28 kHz and 61.87 kHz have been found (Fig. 2). The modal shape at 30.28 kHz combines 1st longitudinal and 4th flexural mode and modal

shape at 61.87k Hz 2nd longitudinal and 6th flexural modes. Combination of the modes strongly depends on actuator's *h/l* ratio and preloaded mass value. Flexural mode number decreases when *h/l* ratio or preloaded mass increases.

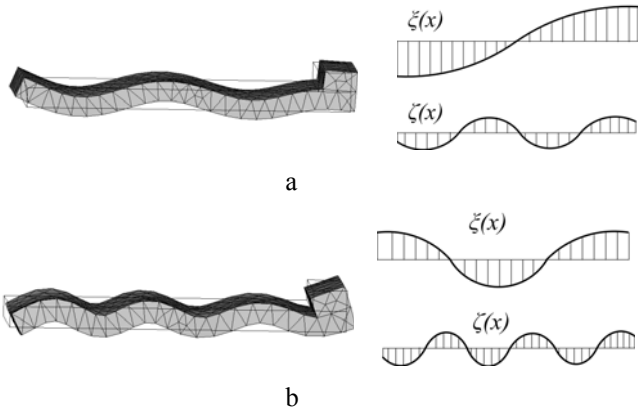

Fig. 2 Modal shapes of the actuator at: a) 30.28 kHz b) 61.87 kHz

Harmonic response analysis was performed with the aims to find out the actuator's response to sinusoidal voltage applied on electrodes of the piezoceramic element, to verify operating principle and to calculate trajectories of arbitrary contact point movement. Contact point is located at the end line of top surface of the actuator (Fig. 1, a). Two excitation schemes were used in the simulations to achieve direct and reverse motion. Principles of excitation schemes are described in Section 2. A 30V AC signal was applied to electrodes. Two frequency ranges from 20 kHz to 40 kHz and from 50 kHz to 70 kHz with a solution at 100 Hz intervals were chosen for the simulation and adequate response curves of contact point's oscillation amplitudes and phases were calculated. The first and the second excitation schemes were used for aforementioned frequency intervals respectively.

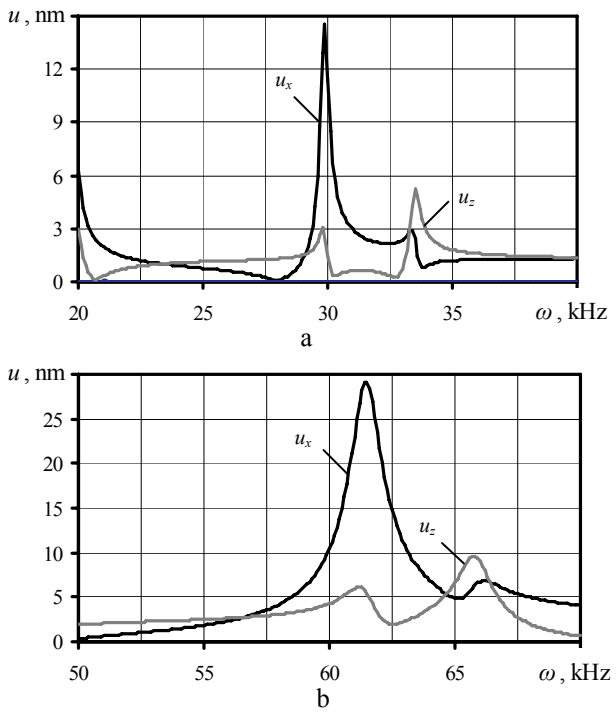

Fig. 3 Amplitude-frequency characteristic of contact point: a) 20-40 kHz interval; b) 50-70 kHz interval

Results of calculations are given in Fig. 3 where amplitude projections u_x and u_z of the contact point's vibration versus frequency are given. These projections correspond longitudinal and flexural vibrations respectively. By examining graphs of contact point's oscillation amplitudes (Fig. 3) it can be seen that local peaks are achieved at the frequencies 29.9 kHz and 61.5 kHz. These frequency values are close to natural frequencies found during modal frequency analysis. Vibration shapes of the actuator at these resonant frequencies are given in Fig. 4.

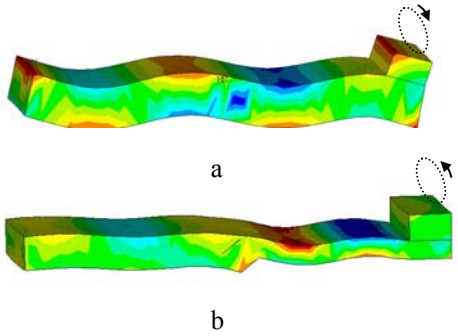

Fig. 4 Vibration shapes of the actuator at: a) 29.9 kHz; b) 61.5 kHz

Calculations of the contact point's moving trajectories were done applying the same two excitation schemes at the frequencies 29.9 kHz and 61.5 kHz accordingly. Fig. 5 illustrates trajectories of the contact point's movement. It can be seen that trajectories have ellipsoidal shapes. Parameters of the ellipses are given in Table 1.

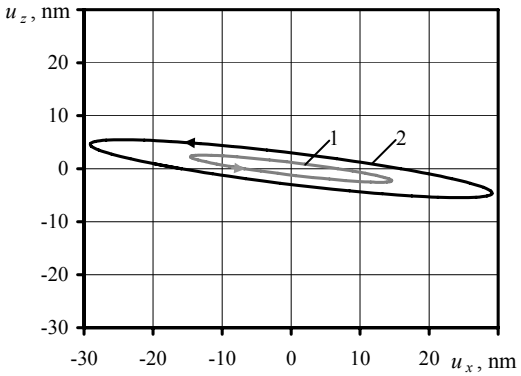

Fig. 5 Trajectories of the contact points motion at: *1* – 29.9 kHz, *2* – 61.5 kHz

Table

Parameters of ellipses

Frequency ω, kHz	Length of major semiaxis L, nm	Ratio between semiaxes	Rotation angle α, degree
29.9	14.74	6.94	-8.67
61.5	28.87	4.21	-10.27

By observing elliptical trajectories and their parameters it can be concluded that trajectories of contact point has opposite directions at different frequencies. It means that slider will have direct and reverse motion at these frequencies. Ellipsis at 61.5 kHz has a 1.8 time larger major semiaxis and bigger area then at 29.9 kHz. It means that the contact point's motion and the strike, respectively, are more powerful at 61.5 kHz than at 29.9 kHz. Fig. 5 shows that attack angle at 29.9 kHz is fairly large, so the strike will be relatively small at this frequency.

Further numerical investigation of piezoelectric actuator was carried out with the task to analyze the influence of preloaded mass on the parameters of elliptical motion of the contact point. Parameters of elliptical trajectories when the ratio of preloaded mass and the mass of piezoceramic beam m_{pr}/m varies from 0.025 till 0.25 were analyzed. Multimode resonant frequencies with dominated 1st and 2nd longitudinal vibration modes were recalculated for each different values of preloaded mass, as resonant frequency of the actuator depends on preloaded mass (Eq. 11). Results of calculations that are ellipses of contact point motion and parameters of the ellipses are given in FigS. 6-8 when different vibration modes are used.

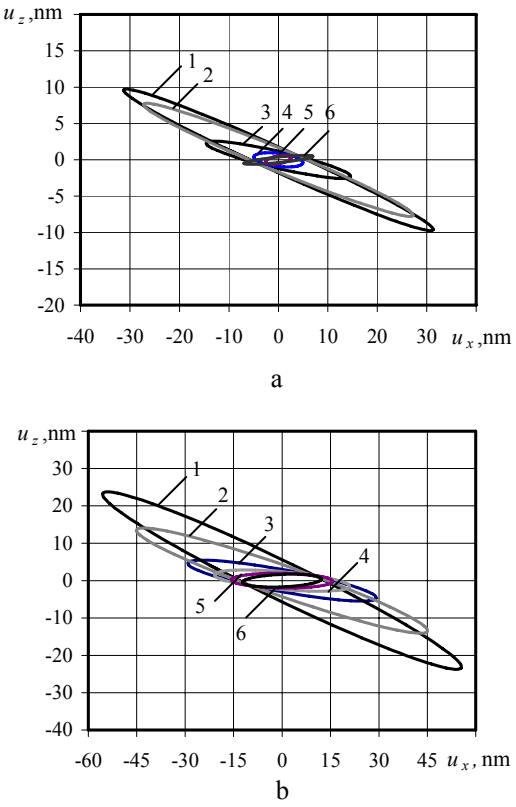

Fig. 6 Trajectories of the contact point motion when different m_{pr}/m is applied: a) multimode vibrations with 1st longitudinal mode, b) multimode vibrations with 2nd longitudinal mode: *1* – $m_{pr}/m = 0.025$, *2* – $m_{pr}/m = 0.05$, *3* – $m_{pr}/m = 0.01$, *4* – $m_{pr}/m = 0.015$, *5* – $m_{pr}/m = 0.02$, *6* – $m_{pr}/m = 0.25$

By observing ellipses (Fig. 6) and parameters of the ellipses presented as a function of the ratio between preloaded mass and piezoceramic beam and m_{pr}/m (Figs. 7, 8) it can be noticed that the length of major semi axes in both vibration modes decreases when ratio m_{pr}/m increases and approaches to the 10 nm (Fig. 7). This means that inertia force at the beam end with preloaded mass increases and vibration amplitudes of the contact point are suppressed. The similar effect is demonstrated in Fig. 8, where rotation angles of the major semiaxes of the elliptical trajectories approach to 0 value when preloaded mass increases. It indicates that flexural component of contact point vibrations decreases while the component of longitudinal vibrations dominates.

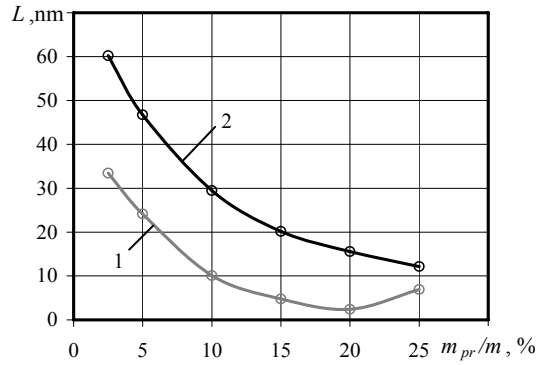

Fig. 7 Length of major semiaxis of ellipses presented as a function of m_{pr}/m: *1* – multimode vibrations with 1st longitudinal mode, *2* – multimode vibrations with 2nd longitudinal mode

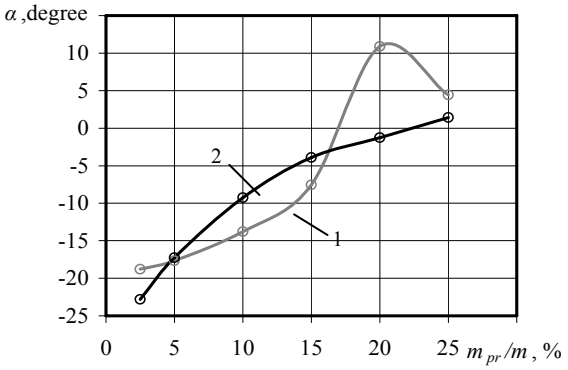

Fig. 8 Rotation angle of major semiaxis of ellipses presented as a function of m_{pr}/m: *1* – multimode vibrations with 1st longitudinal mode, *2* – multimode vibrations with 2nd longitudinal mode

5. Conclusions

Results of numerical modeling and simulation of piezoelectric actuator with preloaded mass were presented in the paper. It was shown that elliptical trajectories of contact point motion can be achieved applying different mass values and different multimode resonant vibrations. Direct and reverse motion of the actuator is obtained using two different multimode vibrations and actuation schemes of the electrodes respectively. Area and the length of major semiaxis of ellipses obtained applying these two multimode resonant vibrations differ, so driving forces of the actuator are different at these modes as well. Parameters of the elliptical trajectories strongly depend on the preload mass value.

Acknowledgement

This work has been supported by Lithuanian State Science and Studies Foundation, Project No. B-07017, "PiezoAdapt", Contract No K-B16/2008-1.

References

1. **Uchino, K., Giniewicz, J**. Micromechatronics. -New York: Marcel Dekker Inc., 2003.-504p.
2. **Uchino, K**. Piezoelectric Actuators and Ultrasonic Motors. -New York: Springer, 1997.-364 p.
3. **Uchino, K.** Piezoelectric ultrasonic motors: overview.

-J. of Smart Materials and Structures, v.7, 1998. p.273-285.
4. **Limanauskas, L., Nemčiauskas, K., Lendraitis, V., Mizarienė, V.** Creation and investigation of nanopositioning systems. -Mechanika. -Kaunas: Technologija, 2008, Nr.3(71), p.62-65.
5. **Bansevicius, R., Barauskas, R., Kulvietis, G., Ragulskis, K.** Vibromotors for Precision Microrobots. Hemisphere Publishing Corp., USA, 1988.-310p.
6. **Hemsel, T., Wallaschek, J.** Survey of the present state of the art of piezoelectric linear motors. -Ultrasonics, v.38, 2000, p.37-40.
7. **Bolotin, V.** Vibrations in Technology. -Moscow: Mashinostrojenije, v.1, 1979.-357p. (in Russian).
8. **Filipov, A.** Oscillations of Deformable Systems. -Moscow: Mashinostrojenije, 1970.-733p. (in Russian).
9. **Lin-nan, Z., Zhi-fei, S.** Analytical solution of a simply supported piezoelectric beam subjected to a uniformly distributed loading. -Applied Mathematics and Mechanics, v.24, No.10, 2003, p.1215-1224.
10. **Safari, A., Akdogan, E. K.** Piezoelectric and Acoustic Materials for Transducer Applications. -New York: Springer, 2008.-540p.
11. **Vasiljev, P., Tiškevičius, J., Mažeika, D., Kulvietis, G.** Piezoelectric actuator for body positioning in the plane. -Mechanika. -Kaunas: Technologija, 2003, Nr.5(43), p.39-43.
12. **Vasiljev, P., Mažeika, D., Kulvietis, G.** Modelling and analysis of omni-directional piezoelectric actuator. -J. of Sound and Vibration, v.308, Issue 3-5, Elsevier, 2007, p.867-878.

D. Mažeika, R. Bansevičius

STRYPINIO PJEZOELEKTRINIO KEITIKLIO SU PAPILDOMA MASE REZONANSINIŲ VIRPESIŲ FORMŲ TYRIMAS

R e z i u m ė

Straipsnyje pateikiami strypinio pjezoelektrinio keitiklio daugiamodalinių virpesių skaitinio tyrimo rezultatai. Nagrinėjamąjį keitiklį sudaro pjezokeraminis strypas su papildoma mase viename strypo gale. Keitiklio elektrodai išdėstyti išilgai strypo ir padalyti į dvi lygias sekcijas. Keitiklis sužadinamas naudojant daugiamodalines, t. y. išilginių ir lenkimo virpesių, formas. Tiesioginiam ir atgaliniam keitiklio judesiui gauti naudojami du skirtingi rezonansiniai dažniai ir dvi elektrodų žadinimo schemos. Naudojant baigtinių elementų metodą buvo sukurtas keitiklio skaitinis modelis, surastos reikiamos daugiamodalinės rezonansinės formos, apskaičiuotos kontaktinio taško judesio trajektorijos. Skaitinio tyrimo metu nustatyta papildomos masės įtaka keitiklio virpesių formoms ir kontaktinio taško elipsinių trajektorijų parametrams.

D. Mažeika, R. Bansevičius

STUDY OF RESONANT VIBRATIONS SHAPES OF THE BEAM TYPE PIEZOELECTRIC ACTUATOR WITH PRELOADED MASS

S u m m a r y

Results of numerical modeling and simulation of multimode resonant vibrations of the beam type piezoelectric actuator are presented in the paper. The investigated actuator consists of piezoceramic beam with a single mass at one of the ends. Electrodes pattern has two sections and two schemes of excitation are used. Operation of the actuator is based on using multimode resonant vibrations where superposition of longitudinal and flexural modes is used. Two separate resonant vibration modes and electrode excitation schemes are used for direct and reverse motion of the actuator. Numerical modeling based on the finite element method was performed to find multimode resonant frequencies and modal shapes and to calculate the trajectories of contact point movement under different excitation schemes. Results of numerical simulation demonstrate the influence of preloaded mass on vibration shapes and parameters of the trajectories of contact point movement.

Д. Мажейка, Р. Бансявичюс

ИССЛЕДОВАНИЯ ФОРМ КОЛЕБАНИЙ СТЕРЖНЕВОГО ПЬЕЗОЭЛЕКТРИЧЕСКОГО ПРЕОБРАЗОВАТЕЛЯ С ДОПОЛНИТЕЛЬНОЙ МАССОЙ

Р е з ю м е

В настоящей работе приведены результаты численного исследования многомодальных колебаний пьезоэлектрического преобразователя. Исследуемый преобразователь состоит из пьезокерамического стержня с дополнительной массой на одном из его концов. Электроды преобразователя расположены по длине стержня и поделены на две равные части. Преобразователь возбуждается применяя многомодальные формы колебания. Для прямого и обратного движении применяются две разные резонансные частоты и две схемы возбуждения электродов. Применяя метод конечных элементов была создана численная модель, найдены необходимые многомодальные резонансные формы колебаний, траектории движения контактной точки и определено влияние дополнительной массы на формы колебаний преобразователя и параметры эллиптической траектории движения контактной точки.

Received December 19, 2008
Accepted March 12, 2009

DOI: 10.5755/j02.mech.15201